ADVANCED OPTICAL MATERIALS
www.advopticalmat.de

Conjugated Polymer Blends for High Contrast Black-to-Transmissive Electrochromism

*Lisa R. Savagian, Anna M. Österholm, Dwanleen Eric Shen, Dylan T. Christiansen, Michael Kuepfert, and John R. Reynolds**

Next-generation electrochromic technologies, such as dimmable fenestration, eyewear integrated displays, and optical shutters require materials that reversibly transition between highly transmissive and broadly absorbing achromatic states, often with minimal intermediate coloration. In this work, it is shown how the properties of dioxythiophene-based electrochromic polymers (ECPs) can be leveraged through straightforward color mixing to yield high-contrast, black-to-transmissive materials with low driving voltages (<1 V), extended functional lifetimes, and minimal transient chromaticity. Drawing from a family of five soluble colored-to-colorless switching polymers (including ECP-cyan, -green, -magenta, -yellow, and a newly reported ECP-orange), three unique cathodically coloring polymer blends are reported, with achromatic neutral states ($C^*_{ab} < 5$) and integrated optical contrast exceeding 40% across the entire visible spectrum (380–780 nm). By incorporating different high-gap and dual-band absorbing ECPs, subtle control is demonstrated over both the extreme and intermediate coloration of the blends. This work showcases how solution coprocessing of ECPs can be used to access highly targeted achromatic hues while also enabling fine-tuned neutral optical transition between black and transmissive states.

1. Introduction

Electrochromic materials that reversibly switch between black and transmissive states are highly sought-after in a number of commercial and military applications, including energy-saving dimmable windows, user-controlled protective eyewear, and optical privacy shutters. In addition, black electrochromes are useful for communicating text and complex images via reflective displays in electronic paper devices, wearable "smart glasses," and transmissive panel monitors. Essential to the utility of such materials is the ability to repeatedly transition between two optical states in a rapid, on-demand fashion.

π-Conjugated electrochromic polymers (ECPs) are a class of electrochromic materials that offer an appealing platform for the realization of true black-to-transmissive electrochromism. ECPs can undergo full colored-to-colorless transitions on rapid time scales (often in second to sub-second regimes,[1] with high coloration efficiencies, contrasts ($\Delta\%T$ at λ_{max}) up to 70%, switching stability over thousands to hundreds of thousands of cycles, and in many cases, colorless states that can be refreshed by a small current or voltage pulse.[1,2] Moreover, ECPs can be readily tuned for color through straightforward chemical modification of the polymer backbone. The addition of solubilizing aliphatic or polar side chains allows for these materials to be processed as electronic inks in low-cost and large-scale processing techniques, such as inkjet-printing, along with blade-, spray-, and slot die coating.[3–10] In recent years, a deeper understanding of the structure–property relationships that control the color and switching properties of ECPs has enabled the development of extensive libraries of cathodically coloring polymers. These materials have been successfully integrated into plastic[5,11,12] and paper-based[7,13,14] electrochromic devices, making them promising candidates for flexible or transient electronic displays.

While most colored-to-transmissive ECPs have π-electronic structures that have been carefully modified to absorb specific wavelengths of visible light for achieving highly saturated colors, a black ECP must absorb across the entire visible spectrum in its colored state. Meanwhile, the transmissive state of the material must absorb as little visible light as possible in the same wavelength range for optimal contrast and optical clarity. Developing a material that undergoes such drastic spectral changes upon application of an electrical bias presents a unique materials design challenge. An additional complexity arises when seeking to develop black-to-transmissive electrochromic materials that are able to transition through intermediate shades of gray, as well.

L. R. Savagian, Dr. A. M. Österholm, Dr. D. E. Shen, D. T. Christiansen, Prof. J. R. Reynolds
School of Chemistry and Biochemistry
School of Materials Science and Engineering
Center for Organic Photonics and Electronics
Georgia Tech Polymer Network
Georgia Institute of Technology
Atlanta, GA 30332-0400, USA
E-mail: reynolds@chemistry.gatech.edu
M. Kuepfert
Re-synthesis Laboratory
NC/IS
BASF Corporation
Tarrytown, NY 10591, USA
The ORCID identification number(s) for the author(s) of this article can be found under https://doi.org/10.1002/adom.201800594.

DOI: 10.1002/adom.201800594

A number of strategies have been invoked in pursuit of black-to-transmissive ECPs. Synthetic approaches have targeted polymers with backbones designed for broad absorption of visible light. Beaujuge et al. reported the first black-to-transmissive ECP using a cathodically coloring random copolymer of 3,4-propylenedioxythiophene (ProDOT) donor and 2,1,3-benzothiadiazole (BTD) acceptor moieties.[15] Two properties of this polymer led to broad absorption across the visible region. First, BTD-based donor–acceptor polymers are characterized by a dual absorbance at long and short wavelengths, which inherently absorb more visible light than most traditional all-donor polymers that exhibit single absorbance bands. Second, the random nature of the copolymerization leads to varying combinations of donor and acceptor along the polymer backbone, each of which absorb in different regions of the visible spectrum. Further optimization of the donor-to-acceptor feed ratio yielded a black-to-transmissive ECP (herein referred to as "ECP-black") that absorbed most broadly across the visible range.[16] This so-called "donor-acceptor approach," which involves copolymerizing electron-poor and electron-rich monomers, has since been employed to yield other black ECPs.[17–19] Broad absorption across the visible range has also been achieved in alternating donor–acceptor polymers by incorporating multiple acceptors along the backbone, such as benzoquinoxaline, benzoselenadiazole, and benzotriazole.[20] Beyond donor–acceptor systems, cobalt-based supramolecular metallopolymers have been pursued as black electrochromes. A salient example involves a Co(II)–bisterpyridine metallosupramolecular polymer that switches between a highly transmissive, pale yellow neutral state and a broadly absorbing darkened state upon electrochemical reduction.[21] Another interesting approach was demonstrated by Sassi et al. in 2016, where a small molecule Weitz-type chromophore that absorbs at short wavelengths, was tethered onto an ethylenedioxythiophene (EDOT)-ProDOT copolymer that absorbs at longer wavelengths. When used in conjunction with a Prussian Blue counter electrode, this material yielded a black-to-clear electrochromic device.[22] A final family of materials that has demonstrated broadly absorbing colored states are triphenylamine (TPA)-based polymers. Both the ProDOT-based polymers described above and TPA electrochromes are p-type materials that switch between a neutral and oxidized state. However, when compared to ProDOT-based polymers, the spectra of TPA polymers are significantly blueshifted due to their shorter effective conjugation lengths. As a result, neutral TPA polymers often absorb in the UV and appear highly colorless, and upon oxidation, they absorb broadly in the visible range upon and appear black. On the other hand, cathodically-coloring ProDOT-based materials appear colored in the neutral state and, upon oxidation, absorb broadly in the NIR and appear transmissive. Through structural tuning, a TPA-based polymer with a black oxidized state and a colorless neutral state was recently developed.[23] Despite this progress, many of these systems do not offer sufficiently broad spectral coverage, especially in the high- and low-energy ranges of the visible region. In particular, cathodically coloring systems like poly(ProDOT)s often suffer from the infrared absorption of the oxidized chromophore tailing into the visible region, leaving a blue tint in the transmissive state.

Given the challenges associated with developing a color-neutral and high optical contrast material, an alternative approach toward black-to-transmissive electrochromism is to blend vibrantly colored chromophores whose collective absorption entirely covers the visible spectrum. This can, in theory, be accomplished using the three traditional subtractive primaries, cyan, magenta, and yellow (CMY), whose respective absorbance bands span the low-, mid-, and high-energy regions of the visible spectrum, or by two-component combinations of dual-band and midgap absorbers, such as green and magenta. Previous work has demonstrated such color mixing principles in dual or stacked black-to-transmissive electrochromic devices[24–27] as well as by solution co-processing of individual cathodically coloring chromophores into a single optically active layer.[26,28] To demonstrate the ability to finely control hue through color mixing, our group has previously utilized solution co-processing of multicomponent ECP blends to tune the dynamic brown coloration in electrochromic eyewear.[29] This blending approach is also advantageous when targeting black-to-transmissive switching, as it allows for facile tuning of optical properties without requiring new material synthesis or complex electrode architectures. In particular, solution coprocessing offers a great deal of versatility and predictability and can readily be adapted to yield different hues of black (e.g., charcoal or noir) by simply tuning the mass ratios of the constituent ECPs.

Blending electrochromes for black-to-transmissive switching, however, demands special consideration of how the optical evolution proceeds with applied electrochemical potential. For applications such as dimmable fenestration and eyewear, where it is desirable to dial in intermediate shades, bleaching and coloration should proceed through color-neutral gray tones, rather than vibrantly colored intermediates. Developing an ECP blend with such properties requires that the consitutent chromophore bleach within a similar voltage window and in a concerted fashion. However, because the color of an ECP is determined by the effective conjugation length and the extent of π orbital overlap in response to various steric and electronic effects, any attempt to manipulate the color will often also result in a change in the electrochemical properties of the material. Consequently, while it may be relatively straightforward to find a combination of ECPs whose collective absorption profiles cover the visible range, it is much more challenging to also ensure that the redox properties of the components coordinate to bleach and color at identical potentials and similar rates. To date, no study has demonstrated how to control both the extreme and intermediate coloration of black-to-transmissive ECP blends.

In this work, solution coprocessing is presented as a means for overcoming the many challenges associated with high-contrast black-to-transmissive electrochromism. We demonstrate how the composition of ECP blends can be strategically tailored to access a range of black hues with complete coverage of the visible spectrum, enhanced redox stability, and achromatic optical transitions to highly transmissive states. Utilizing a collection of five soluble ProDOT-based copolymers, we present an expanded subtractive color mixing approach beyond the traditional CMY model and report a series of three-component black ECP blends. By including a green and a new orange colored-to-colorless polymer in our mixing scheme, we can control the colored states, intermediate hues, and long-term coloration of black-to-transmissive ECP films. With integrated contrast across the visible spectrum exceeding 40%, these materials are significantly more color-neutral than our previously reported ECP-black and can be tuned for achromatic optical transitions.

2. Results and Discussion

2.1. Electrochromic Properties of ECP Blends

Because the perception of color is highly subjective, it is important to be able to quantify the exact hue of various colors for valid comparisons. The human eye has three types of cone cells that are sensitive to unique wavelength ranges of light; if the total spectral power distribution of light is weighted to account for this relative sensitivity, three effective stimulus values are generated. These three values can objectively quantify a color.[30] Quantification of chromaticity can be accomplished in the CIELAB coordinate system, where a 3D vector space defines the chromaticity and luminosity of a color. Here, L^* represents the lightness of a color, where 0 is black and 100 is diffuse white. The a^* and b^* axes (+/−128) represent the relative saturation of four quaternary colors: red ($+a^*$), green ($-a^*$), blue ($-b^*$), and yellow ($+b^*$). A vibrant color with high degree of saturation will have large a^* and/or b^* values, such as Coke Red ($L^* = 53$, $a^* = 80$, $b^* = 59$).[31] A truly achromatic color (e.g., black, gray) can be accessed when a material's absorbance, combined with the nonlinear spectral sensitivity of the human eye, completely and uniformly attenuates the intensity of all visible light. Achromatic shades have relatively equal contributions from each of the four chromatic components and therefore map to low (a^*, b^*) coordinates (i.e., a^* and b^* values close to 0). A black-to-clear electrochromic material with intermediate gray shades would ideally only exhibit a variation of L^* upon switching. The color chromaticity (C^*_{ab}) represents the overall hue of the color and is defined as the magnitude of the vector in the (a^*, b^*) plane, as indicated by Equation (1). Color-neutral shades (e.g., black and gray) have equal contributions from each of the quaternary chromatic components and therefore are associated with low C^*_{ab} values.

$$C^*_{ab} = \sqrt{(a^*)^2 + (b^*)^2} \quad (1)$$

When blending polymers to achieve a color neutral black, five dioxythiophene-based polymers were selected from our group's collection of colored-to-colorless ECPs. These ECPs readily dissolve in toluene and can be co-processed from solution into homogeneous electrochromic films. Each blend was formulated to include a high-gap absorber (ECP-yellow or -orange), a midgap absorber (ECP-magenta), and dual-band chromophore with strong absorption bands in both the low- and high-energy ends of the visible spectrum (ECP-cyan or -green). Not only does this color mixing scheme offer a means toward materials with broad spectral coverage in the colored state, but it also allows for the high-, mid-, and low-energy absorption intensity of the blend to be independently manipulated, which is important when fine-tuning the blend composition to a desired achromatic state. In addition, we show that by varying the blend components we are able to manipulate the intermediate colored states and the switching performance. Following this model, three different black blends were formulated: a conventional CMY blend (comprising ECP-cyan, -magenta, and -yellow), a CMO blend (ECP-cyan, -magenta, and -orange), and a GMO blend (ECP-green, -magenta, and -orange), as shown schematically in **Figure 1**.

The redox and optical properties of the individual blend components are summarized in **Table 1**, with the corresponding spectra and redox characterizations shown in **Figure 2** as well as Figures S1 and S2 in the Supporting Information. Figure 2A–C shows the neutral state spectra of the individual ECPs as well as their composite blend spectra, and Figure 2D compares the cyclic voltammograms of the blend components. The noteworthy differences between the two high-gap absorbers (ECP-yellow and ECP-orange) and the two low-gap absorbers (ECP-green and ECP-cyan) are the onset of oxidation (E_{onset}, determined by differential pulse voltammetry (DPV) as shown in Figure S1 of the Supporting Information) and the potential required to reach the transmissive state (E_{clear}). These differences, as we will demonstrate, have a substantial impact

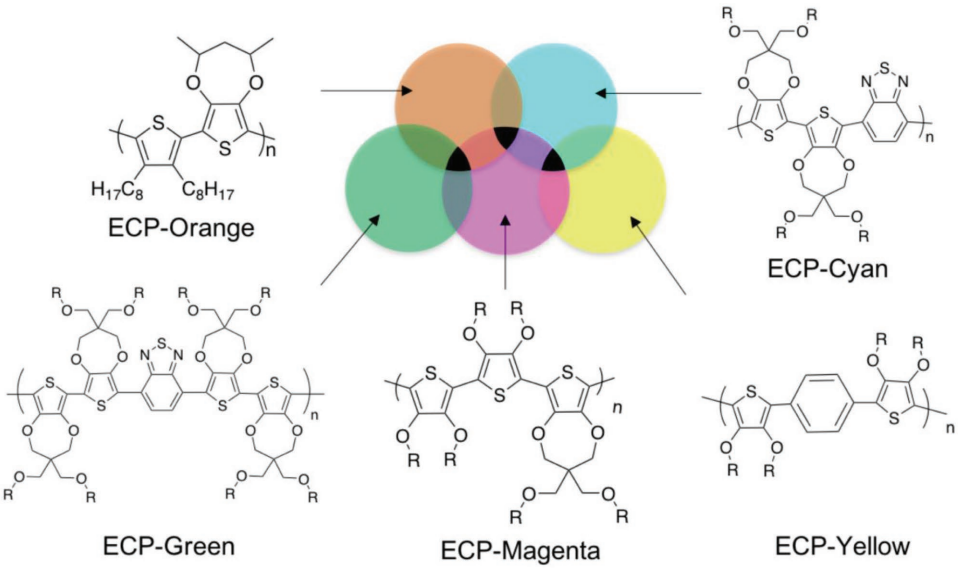

Figure 1. Repeat unit structures of ProDOT-based conjugated electrochromic copolymers used for blending and schematic of subtractive mixing strategies for accessing black. R = 2-ethylhexyl.

Table 1. Redox and optical properties of ECPs used in blends.

ECP	λ_{max} [nm]	E_{onset} [V] vs Fc/Fc^+	E_{clear} [V] vs Fc/Fc^+	a^*, b^*	Contrast at λ_{max} (%)[a]
ECP-yellow	465	0.47	0.7	9, 76	60
ECP-orange	468	0.18	0.5	29, 68	65
ECP-magenta	544	0.12	0.3	59, −16	70
ECP-cyan	406, 687	0.22	0.6	−30, −15	50[b]
ECP-green	458, 672	0.13	0.5	−36, 2	50[b]

[a]Contrast is measured for films coated to a transmittance of 10% +/−2% at λ_{max}; [b]For ECP-cyan and ECP-green, contrast was measured at the low-energy absorbance band.

on the electrochromic switching properties and intermediate coloration of blended ECPs. E_{clear} is determined spectroscopically and corresponds to the potential above which we observe no further change in the level of transmittance in the visible range upon further oxidation. The potential-dependent absorption spectra for the various blend components used in this study are shown in Figure S2 of the Supporting Information.

ECP-yellow and ECP-orange have similar λ_{max} values, but ECP-orange is slightly more broadly absorbing, as shown in Figure 2 (a direct comparison can be found in Figure S3a of the Supporting Information). This spectral difference, though minor, results in a significant difference in perceived color. This can be explained by the photopic response of the human eye. The increased spectral coverage of ECP-orange encompasses a region of the visible spectrum where the human eye is most sensitive to changes in the wavelength (≈480–520 nm). Therefore, subtle differences on the low-energy side of the absorbance spectra of ECP-orange and ECP-yellow are exaggerated when these materials are viewed by the human eye, resulting in noticeably different colors. This is reflected by the large difference in the a^* values associated with the reduced states of the two ECPs (Table 1).

When comparing the redox properties of ECP-orange and ECP-yellow, the difference in oxidation potential arises from a combination of both steric and electronic effects. In ECP-yellow, the high degree of aromaticity of the benzene ring and the bulkiness of the ethylhexyloxy groups obstruct planarization to a quinoidal geometry in the oxidized state, giving rise to the high E_{onset} (Figure 2D) and E_{clear} (Figure S2, Supporting Information). The 3,4-dioctylthiophene comonomer used in ECP-orange, on the other hand, is inherently easier to oxidize than the phenylene unit in ECP-yellow due to the decreased aromatic stabilization associated with the thiophene heterocycle. This results in a higher HOMO (highest occupied molecular orbital) energy and, consequently, a lower E_{onset}. By replacing the 3,4-alkoxy functionalized thiophene units in ECP-yellow with 3,4-propylenedioxy-functionalized analogs in ECP-orange, the functional groups are further away from the conjugated backbone, which also decreases the steric hindrance obstructing planarization. The backbone of ECP-orange, being exclusively composed of thiophene-based repeat units, also allows for an anti configuration

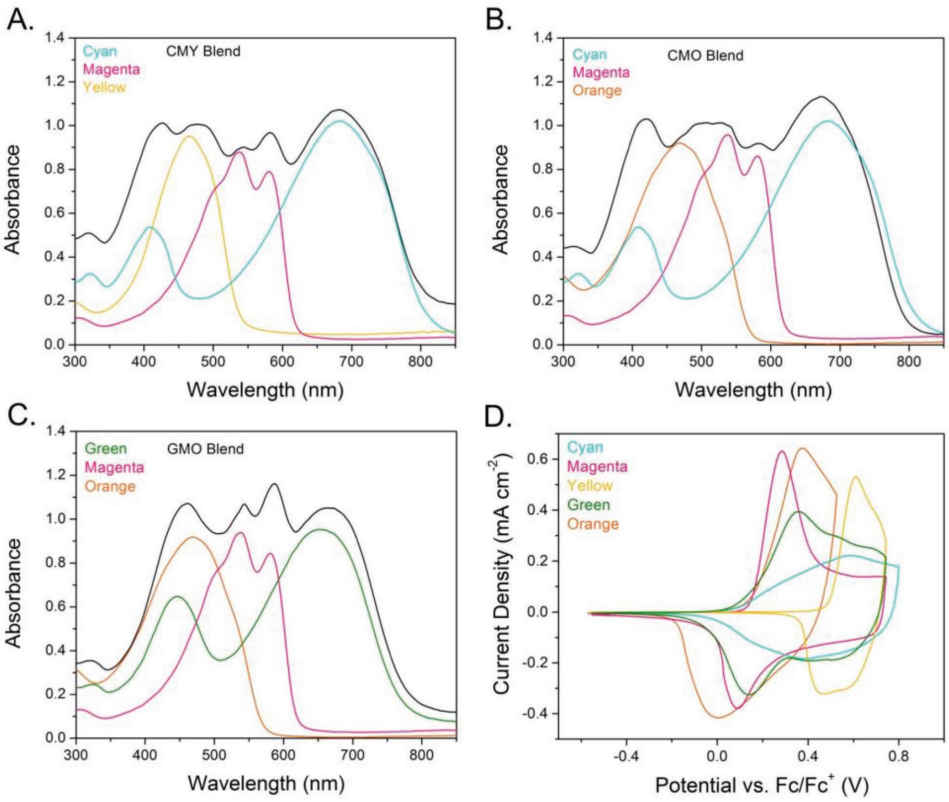

Figure 2. Superimposed absorbance spectra of individual electrochromic polymer components and blends (black lines) of A) cyan–magenta–yellow, B) cyan–magenta–orange, and C) green–magenta–orange. D) Superimposed cyclic voltammograms of ECPs blended in this study, performed on drop-casted films on glassy carbon electrodes in 0.5 M $TBAPF_6$/PC.

between rings, i.e. the 3,4 positions between neighboring rings are antiperiplanar, which in turn reduces inter-ring strain and allows for greater backbone planarization in the neutral state when compared to ECP-yellow. Additionally, this allows the oxidized state of ECP-orange to more easily assume a quinoidal-type bonding structure and therefore exhibit a lower E_{clear} relative to ECP-yellow.

When evaluating the two low-gap components, ECP-green and ECP-cyan, the difference in E_{onset} is the result of the higher relative ratio of the electron-rich (ProDOT) to the electron-poor (BTD) moieties in ECP-green. This increase in electron-richness destabilizes the HOMO level of ECP-green relative to ECP-cyan, resulting in a decreased E_{onset}, as well as cathodically shifted redox peaks in the cyclic voltammograms, as shown in Figure 2D. The higher ProDOT content in ECP-green also facilitates planarization and charge carrier delocalization, leading to a 0.1 V lower E_{clear} (Table 1). The optical properties of ECP-cyan and ECP-green are fairly similar, as both exhibits a dual-band absorbance profile characteristic of many donor–acceptor polymers. The band at longer wavelengths arises from a transition between a delocalized HOMO and a LUMO (lowest occupied molecular orbital) localized on the acceptor, while the short wavelength absorption band originates from a transition between the HOMO and the LUMO+n orbital localized on the donor unit.[32] By increasing or decreasing the donor content in the ECP backbone, the position of the high-energy band can be readily red- or blueshifted, whereas the low energy band is less sensitive to the donor–acceptor ratio. The higher ProDOT content in ECP-green results in a redshifting of the high-energy band of this ECP by about 50 nm relative to ECP-cyan, whereas the low energy band is blueshifted only by 15 nm. This significant shifting of the high-energy band results in ECP-green absorbing more in the middle of the visible spectrum (450–500 nm) and less at the extremes when compared to ECP-cyan.

To make color-neutral blends, the relative amount of each ECP was adjusted such that resulting films exhibited relatively uniform spectral coverage and low chromaticity ($C^*_{ab} < 5$) in the colored state (Figure 2 and **Table 2**). As shown in Table 2, each of the three-component ECP blends are significantly more color neutral than the random copolymer ECP-black ($C^*_{ab} = 16$) which has a slight purple hue and a higher negative b^* (see comparison in **Figures 3**A and **4**).

Table 2. Color coordinates and color saturation of evaluated ECP blends and ECP-black.

Material		Mass ratios	Colored state				Transmissive state			
			L^*	a^*	b^*	C^*_{ab}	L^*	a^*	b^*	C^*_{ab}
Blends	CMY	10-4-2	45.1	2.5	−1.0	2.7	82.1	−7.1	−1.5	7.3
	CMO	10-4-4	40.1	4.4	−1.3	4.6	81.5	−4.7	−4.8	6.7
	GMO	10-3.4-1	37.7	−1.7	−2.8	3.3	81.7	−4.6	−6.1	7.6
ECP-Black		–	40.0	−3.1	−15.7	16.0	84.2	−5.4	−4.7	7.1

The enhanced color neutrality of the CMY, CMO, and GMO blends can be attributed to their broadened and more uniform absorbance across the visible spectrum, especially below 450 nm and above 750 nm, where these blends absorb more effectively than ECP-black (Figure 3A). The different ratio of blend components is due to subtle differences in the absorbance spectra of each of the ECPs. For instance, when comparing CMY with CMO, the absorption band of ECP-orange is broader with respect to that of ECP-yellow, so the CMO blend requires less of the mid-gap chromophore ECP-magenta to achieve color neutrality. Similarly, the high-energy absorption band of ECP-cyan is blueshifted relative to that of ECP-green. As a result, in the GMO blend the absorbance of ECP-orange and the high-energy band of ECP-green overlap more closely than ECP-orange and ECP-cyan in the CMO blend. To compensate, the amount of ECP-orange was reduced fourfold in the GMO blend, compared to the CMO blend. Finally, ECP-cyan absorbs more low- and high-energy light than ECP-green, which impacts the blend in two ways. First, because the high- and low-energy absorption bands are brought closer together in ECP-green, slightly less of the midgap absorber (ECP-magenta) relative to the dual-band absorber is required to formulate the GMO blend than the CMO blend. Second, CMO and CMY blends have broader spectral coverage than the GMO blend; however, GMO is still very color-neutral ($C^*_{ab} = 3.3$), as the human eye is least sensitive the light transmitted at the extreme ends of the visible spectrum.

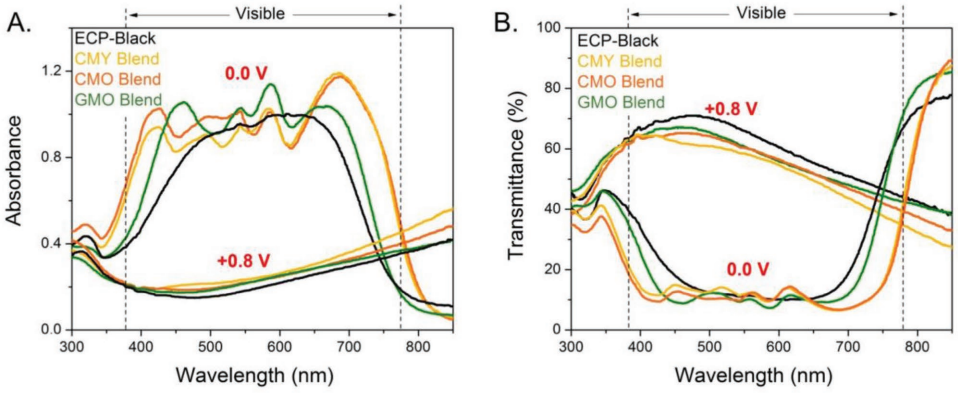

Figure 3. Superimposed A) absorbance and B) transmittance spectra for ECP-black (black lines), CMY black (yellow lines), CMO black (orange lines), and GMO black (green lines) in the oxidized state (+0.8 V) and reduced state (0.0 V). Dashed lines denote the limits of the visible spectrum (380–780 nm).

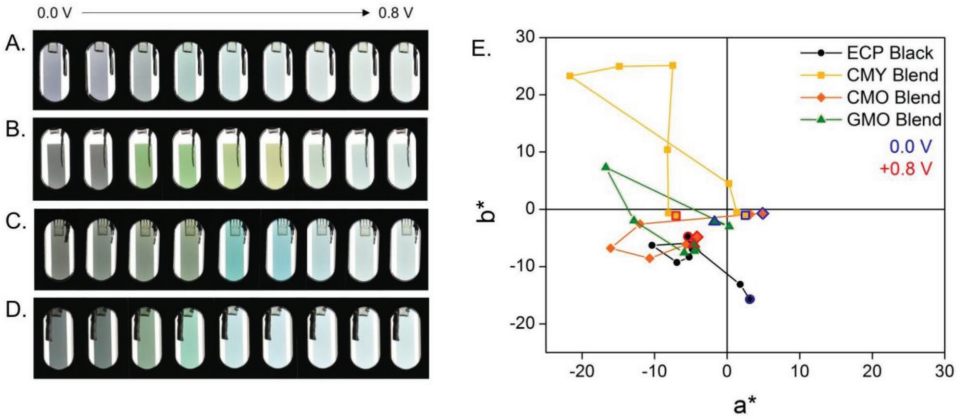

Figure 4. Photographs of A) ECP-black, B) the CMY blend, C) the CMO blend, and the D) GMO blend taken under potentiostatic control. Each photograph is taken at 0.1 V increments, increasing from 0 V to +0.8 V versus Ag/Ag^+ in 0.5 M $TBAPF_6$-PC. E) The corresponding color coordinates for ECP-black and the various blends at 0.1 V increments.

When oxidized to their colorless states, the transmittance spectra of the blends all follow a similar trend across the visible, with each material transmitting the greatest amount of green–yellow light (500–600 nm) as shown in Figure 3B. For electrochromic materials, contrast is often evaluated as the change in transmittance between the reduced and oxidized states at a single wavelength. For broadly absorbing hues like black, it is more descriptive to define contrast as the change in integrated transmittance across the entire visible spectrum, which spans from 380 to 780 nm according to Commission internationale de l'éclairage (CIE) standards.[33] Among the blends, the CMY film has the lowest integrated transmittance in the colorless state, presumably due to the reduced electrochromic contrast of ECP-yellow when compared to ECP-orange, especially above 650 nm (Figure S3a, Supporting Information), as well as the larger relative amount of ECP-cyan. While both the CMO and the GMO can reach a similar level of transmittance in the oxidized state, the higher integrated contrast of the CMO blends is a result of the broader spectral coverage achieved by the colored state of this blend. While ECP-black has the highest integrated transmittance in the oxidized state, it does not have the highest integrated contrast. This can be explained by ECP-black's colored state, which has a relatively narrower absorption profile in the visible range than the blends in the visible region, leading to a higher integrated transmittance at +0.0 V. Each of the blends exhibits an integrated contrast across the entire visible spectrum greater than or equal to that of ECP-black (40%) with the CMO blend having the highest integrated contrast (45%) among all black materials evaluated (see **Table 3**).

While each blend studied has a unique composition, their electrochemical properties do not differ much. As demonstrated in Figure S4 in the Supporting Information, the CMO, GMO, and CMY blends and ECP-black all pass similar amount of current and require a comparable charge to switch between the colored and colorless states (Table 3). Each black formulation undergoes a broad oxidation within a potential window ranging from +0.1 V to 0.8 V. The E_{onset} for each blend occurs around +0.08 V (Table 3), while ECP-black begins oxidizing at 0.02 V versus Fc/Fc^+. Interestingly, the CMY, CMO, and GMO blends all oxidize at slightly lower potentials than the E_{onset} of their constituent ECPs, suggesting that there are intermolecular interactions in these blends that may result in the formation of polymer domains that are more susceptible to electrochemical oxidation. However, a more important property for these cathodically coloring blends is the E_{clear}. As expected, the CMY blend has the highest E_{clear} as a result the ECP-yellow component, which bleaches at the highest electrochemical potential. The GMO blend exhibits the lowest E_{clear} of the blends, which is not surprising, as it comprises the three ECPs with the lowest E_{clear} values. When evaluating the kinetics of the black-to-transmissive transition, the CMO and GMO exhibit similar switching times when stepped between –0.5 and +0.8 V and can complete a full transition in 2 s, as shown in Figure S5 in the Supporting Information. The CMY blend exhibits slightly slower switching kinetics using this same potential step, most likely due to high oxidation potential of ECP-yellow, which has been previously observed for brown ECP blends.[29]

To evaluate the functional lifetimes of the CMY, CMO, and GMO blends, each film was repeatedly stepped between the colored (–0.5 V) and colorless (+0.8 V) state 1000 times. After ≈100 switches, the CMY blend lost almost 10% of its overall integrated contrast (Figure S6, Supporting Information). This loss in contrast is attributed to the electrochemical instability of the ECP-yellow component, which has been demonstrated in previous work.[34] As shown in Figure S7 in the Supporting Information, the *b** value of the CMY blend decreased from about –1.5 to –17 over 1000 switches, corresponding to a loss in yellow chromaticity and increased blue coloration. By substituting

Table 3. Electrochromic and electrochemical properties of black blends and ECP-black. All potentials are reported versus Fc/Fc^+ couple.

	ECP-black	CMY blend	CMO blend	GMO blend
%*T* (+0.8 V)	61	51	56	57
%*T* (0.0 V)	21	11	12	17
Integrated contrast (%)	40	40	45	40
E_{onset} (V)	+0.02	+0.08	+0.08	+0.09 V
E_{clear} (V)	+0.5	+0.7	+0.6	+0.5
Charge to switch (mC cm^{-2})	3.3	4.1	3.6	3.7

ECP-yellow for ECP-orange in the CMO and GMO blends, the switching stability can be greatly improved, as ECP-orange is able to maintain its full optical contrast over 1000 redox cycles (Figure S8, Supporting Information). Over the course of 1000 switches, the CMO and GMO blends exhibit minimal change in overall chromaticity and remain relatively color neutral (Figure S9, Supporting Information), demonstrating that both the CMO and the GMO are robust electrochromic systems.

2.2. Transitional Coloration

By incorporating ECPs with a diverse set of redox properties and coloration kinetics, solution coprocessing offers the unique possibility of directly controlling the chromaticity of the optical evolution. In certain applications, such as for windows or eyewear, it is desirable to be able to access color-neutral intermediate shades. For other uses, such as on–off displays or optical shutters, it is more important that the switch between the extreme states occurs rapidly and with little detectable transient chromaticity. Following this motivation, both the intermediate and transient optical properties of the ECP films were studied.

To study their intermediate chromaticity, the ECP films were incrementally oxidized in 0.1 V steps ranging from 0.0 V (black state) to +0.8 V (transmissive state). At each potential, the visual appearance (Figure 4A), CIELAB coloration (Figure 4B), and spectral composition (Figure S10, Supporting Information) were evaluated. In doing this, we evaluate which colors between the extreme states can be "dialed in" under intermediate potentiostatic conditions. As shown in Figure 4A, ECP-black transitions from a blue–purple color to a transmissive state through light blue intermediates. The color coordinates associated with this process maintain low a^* and b^* values throughout the transition as shown in Figure 4E. In the case of the CMY blend (Figure 4B), the E_{clear} mismatch between ECP-cyan, -magenta, and -yellow results in vibrantly colored intermediate states. At +0.2 V, ECP-magenta has reached a fairly colorless state, while ECP-cyan and ECP-yellow remain fully colored, as evidenced by the strong absorptions bands below 500 nm and above 600 nm in the potential-dependent spectra (Figure S9, Supporting Information). This residual absorption results in the film exhibiting intermediate shades of green with (a^*, b^*) values that deviate greatly from the achromatic origin of the CIELAB color space (Figure 4E). Above +0.6 V, ECP-cyan is oxidized to its transmissive state, leaving ECP-yellow as the only colored component remaining in the film until it finally bleaches at +0.8 V. Similarly, the CMO blend undergoes a strongly colored optical evolution from the black to the transmissive state. In the CMO blend (Figure 4C), ECP-magenta and ECP-orange are oxidized to a transmissive state within a narrow potential window whereas ECP-cyan remains colored until +0.6 V, giving rise to a vibrant cyan intermediate state with L^* = 66, a^* = −16, and b^* = 7 (C^*_{ab} = 17.5) between +0.4 and +0.5 V. ECP-green, on the other hand, having a lower E_{onset} and E_{clear} than ECP-cyan, reaches its colorless state at a potential that more closely aligns with the E_{clear} of ECP-magenta and ECP-orange. Matching the E_{clear} of each ECP component in the GMO blend results in a more concerted bleaching process and a more color-neutral optical evolution. While the color of the GMO film appears slightly green at +0.3 V (L^* = 55 a^* = −16, b^* = 7, C^*_{ab} = 17.5), the overall transition is not nearly as vibrant as the CMY or CMO blends because of the lower L^*. The reason for the residual green hue at +0.3 V is that ECP-magenta (Figure S2, Supporting Information), unlike ECP-green, switches from a vibrantly colored state to a fairly clear state within a narrow potential window, rather than gradually bleaching out as the oxidation process progresses. This result demonstrates that measuring and reporting E_{clear} is perhaps even more important than the E_{onset} especially when developing ECP blends. Because each component in the GMO blend has a relatively low E_{clear}, this formulation reaches a fully transmissive state at +0.5 V, which is much lower than the potentials required to reach similar optical states in the CMY and CMO blends (Table 3).

When switching the blend films rapidly between the reduced and oxidized states (on/off switching), there may also be detectable transitional colors as the film evolves from its extreme black and transmissive states. This transient coloration is determined by not only the redox potentials of each component, but also by the kinetic factors associated with the bleaching of each chromophore. To evaluate the nature of the transitional colors when switching between black and transmissive states, a square wave bias of −0.5 V to +0.8 V was applied to the CMO and GMO films and spectra were recorded every 0.1 s to capture the nature of the direct optical evolution from the black to the transmissive state. For both the CMO and GMO blends, the first 0.4 s after oxidation is associated with a drastic decrease in the absorbance in the mid-range of the visible spectrum (500–550 nm), as shown in **Figure 5**A, as a result of the rapid bleaching of ECP-magenta. In the later stages of bleaching, contributions from ECP-cyan and ECP-orange dominate the spectra of the CMO blend. Because the high-energy band of ECP-cyan does not overlap much with the absorbance of ECP-orange, the combined absorbance of these components results in rather even coverage of the visible spectrum in the later stages (0.5–1.0 s) of the optical evolution. This is illustrated by the colored rectangles in Figure 5, which show the spacing of the ECP-cyan and ECP-orange absorbance bands during the transitional coloration. Because the high-energy absorbance band of ECP-green is redshifted with respect to that of ECP-cyan, the absorption band of ECP-green has a greater overlap with ECP-orange. This can be seen schematically in Figure 5B from 420 to 490 nm, highlighted by the green and orange bars. As a result of this overlap, the spectral evolution assumes a distinct, uneven curvature with reduced absorbance around 500 nm, which indicates that the GMO blend bleaches through slightly green-tinted shades when transitioning directly from the black state. The reduced overlap of these bands in the CMO blend results in a more color-neutral optical evolution from the black to the transmissive state. Once ECP-magenta has reached a colorless state in the GMO blend, the remaining transition is characterized by the bleaching of ECP-green and ECP-orange.

While the intermediate coloration of the GMO blend appears the most color-neutral when applying intermediate electrochemical potentials (Figure 4), here we can see that the GMO black-to-transmissive evolution is slightly more colored than that of the CMO blend when switching in an on/off fashion between extreme potentials. Therefore, a blend similar to

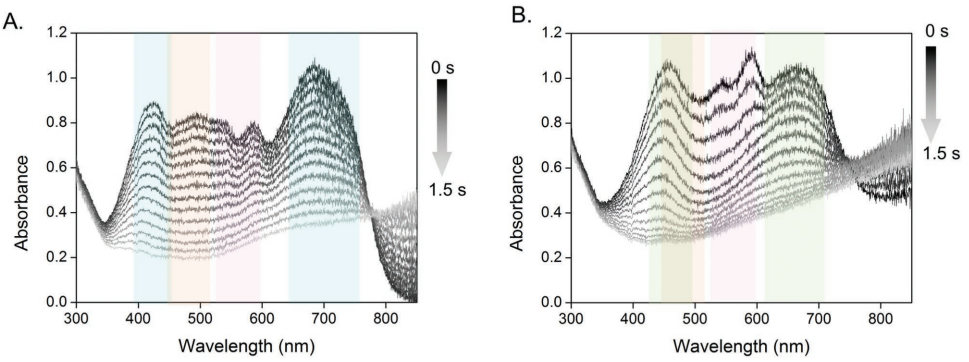

Figure 5. Spectral evolution of A) CMO blend and B) GMO blend when applying a square wave potential from −0.5 V to +0.8 V (vs Ag/Ag^+) in 0.5 M $TBAPF_6$/PC. The black line represents the absorption spectra of the films in the reduced state at the time of the pulse, while the lightest gray line represents the spectra 1.5 s after applying the square wave. Spectra was recorded every 100 ms. Superimposed on the spectra are colored bands corresponding to the absorption maxima and full width at 75% peak maximum of the individual ECP components: ECP-cyan (cyan rectangles), ECP-magenta-2 (pink rectangles), ECP-orange (orange rectangles), and ECP-green (green rectangles).

GMO, where the oxidation potentials are more closely aligned, would be superior for applications in which intermediate achromatic shades need to be accessed or dialed in, or when a lower driving voltage is required. On the other hand, in applications where direct black-to-transmissive transition must exhibit minimal transient coloration, a blend with components whose absorbance bands are spaced further apart, such as the CMO blend, would be more advantageous. The broadened absorbance spectrum can compensate for disparities in the bleaching and coloration of each component.

For truly color-neutral black-to-transmissive switching, the coloration and bleaching kinetics of each chromophore should be similar so that the transition between extreme occurs through achromatic, evenly absorbing intermediate shades. However, factors that govern kinetic characteristics are complex, as they involve migration of both charge carriers and solvated ions that must occur simultaneously and, as a result, may depend on electrolyte properties and the microstructure of the polymer film. Therefore, it is difficult to predictably tune the switching kinetics through structural modifications of the polymer. In ECP blend formulations where one component bleaches at a faster rate than the others (namely, the ECP-magenta component in the CMO and GMO blends), it appears to be advantageous if the chromophores exhibit little spectral overlap, thereby allowing for more even coverage across the visible spectrum throughout the optical transition.

3. Conclusion

Using five vibrant colored-to-colorless dioxythiophene-based polymers and following straightforward color-mixing principles, we have developed new electrochromic polymer blends that reversibly switch between highly desirable black and transmissive states and can be tuned for achromatic optical transitions. These blends include a conventional CMY subtractive combination (ECP-cyan, -magenta, and -yellow), as well as CMO (ECP-cyan, -magenta, and -orange), and GMO (ECP-green, -magenta, and -orange) formulations. Combining the constituent ECPs through scalable solution co-processing techniques allows us to control the precise ratio of the chromophores, predictably balance the chromatic contributions of each component, and access achromatic states ($C^*_{ab} < 5$) that absorb more broadly across the visible spectrum than previously reported single-component donor-acceptor black-to-clear ECPs. By substituting the new ECP-orange for ECP-yellow in the CMO and GMO blends, we can overcome the stability issues associated with the high gap component and produce blends that maintain coloration over hundreds of redox cycles without compromising electrochromic contrast. Owing to the low oxidation potential of ProDOT-rich ECP-green, the GMO blend reaches a transmissive state at a lower potential than the CMO blend (+0.5 compared to +0.6 V vs Fc/Fc^+), exhibits more coordinated bleaching of the constituent chromophores, and transitions through low (a^*, b^*) achromatic intermediates. Utilizing ECP-cyan, which has an inherently broadened absorption spectrum when compared to ECP-green, allows the CMO blend to exhibit more color neutral on/off switching between its extreme black and transmissive states. To achieve truly achromatic and synchronized switching of blended electrochromic materials, such as those described in this study, additional work is needed to understand the kinetic factors associate with ECP coloration and bleaching.

4. Experimental Section

Materials: ECP-black was synthesized with Stille coupling according to a previously published procedure[16] (M_n: 10 kDa; $Đ_M$: 1.6). ECP-magenta (direct (hetero)arylation polymerization, M_n: 11.5 kDa, $Đ_M$: 2.3), ECP-cyan (direct (hetero)arylation polymerization, M_n: 19.8 kDa, $Đ_M$: 4.3), ECP-yellow (direct (hetero)arylation polymerization, M_n: 88 kDa, $Đ_M$: 3.9) were synthesized using previously reported procedures.[29,35] ECP-green and ECP-orange were also synthesized using direct (hetero) arylation polymerization. Synthetic conditions and characterization for these polymers can be found in the Supporting Information.

To fabricate ECP films, all polymers were dissolved at 2 mg mL^{-1} in toluene and spray cast at 20 PSI onto indium tin oxide (ITO)-coated glass slides (Delta Technologies, 8–12 Ω sq^{-1}) to an optical density of 1 ± 0.1 a.u. using an Iwata Eclipse spray gun. To formulate ECP blends, solutions of each ECP (2 mg mL^{-1} in toluene) were combined in the reported ratios (based on solution volume and therefore mass) and spray cast using the same tools. Optical and redox properties were evaluated in 0.5 M tetrabutylammonium hexafluorophosphate ($TBAPF_6$, Acros Organics, 98%, purified by recrystallization from hot ethanol) in propylene carbonate (PC, Acros organics, 99.5%).

Electrochemical and Optical Characterization: Spectroscopic, kinetic, and spectroelectrochemical measurements (integrated contrast, E_{clear}, charge to switch) were performed in a three-electrode cell with a platinum flag as the counter electrode, an Ag/Ag^+ reference electrode (10×10^{-3} M $AgNO_3$ in 0.5 M $TBAPF_6$ (acetonitrile), $E_{½}$ for Fc/Fc^+ couple: +0.065 V), and ECP-coated ITO as the working electrode. The current and voltage were controlled and measured using an EG&G PAR 273A potentiostat/galvanostat under CorrWare control.

For electrochemical characterization, all films were evaluated by cyclic voltammetry (CV, −0.5 V and +0.8 V at 0.050 V s^{-1}) and DPV using a three-electrode cell with a Pt flag as the counter electrode, an Ag/Ag^+ reference electrode (10×10^{-3} M $AgNO_3$ in 0.5 M $TBAPF_6$-ACN, $E_{½}$ for Fc/Fc^+ couple: +0.065 V), and ECP-coated glass carbon working electrode. For these electrochemical measurements, 2 µL of ECP stock solution (2 mg mL^{-1}) were dropcasted on the glassy carbon working electrode (area = 0.07 cm^2) and allowed to dry at room temperature to form a thin film.

The in situ spectroscopic analyses were performed with an Ocean Optics USB2000+ fiber-optic spectrophotometer. The colors of the ECP films were quantified by converting the absorbance spectra to CIELAB (L^*, a^*, b^*) color coordinates where the L^* represents the white–black balance, a^* the green-red balance, and b^* the blue–yellow balance of the color. The photography was performed in a light booth with D50 illumination using a Nikon D90 SLR camera with a Nikon 18–105 mm VR lens. The photographs were reported without any manipulation apart from photograph cropping. For stability studies, ITO was pretreated with hexylphosphonic acid (10×10^{-3} M in ethanol) to prevent film delamination, and film characterization was performed in degassed electrolyte solution under an argon blanket.

Supporting Information

Supporting Information is available from the Wiley Online Library or from the author.

Acknowledgements

This material was based upon work supported by the National Science Foundation Graduate Research Fellowship under Grant No. DGE-1650044 (L.R.S.). The authors gratefully acknowledge funding from NXN Licensing and the Air Force Office of Scientific Research (Grant FA9550–18–1–0184).

Conflict of Interest

The authors declare the following competing financial interest(s): Electrochromic polymer technology developed at the Georgia Institute of Technology has been licensed to NXN Licensing. J.R.R., A.M.O., and D.E.S. served as consultants to NXN Licensing.

Keywords

black electrochromism, color mixing, electrochromic polymers

Received: May 5, 2018
Revised: June 6, 2018
Published online: July 1, 2018

[1] D. E. Shen, A. M. Österholm, J. R. Reynolds, *J. Mater. Chem. C* **2015**, *3*, 9715.
[2] P.-H. Aubert, A. A. Argun, A. Cirpan, D. B. Tanner, J. R. Reynolds, *Chem. Mater.* **2004**, *16*, 2386.
[3] J. Jensen, H. F. Dam, J. R. Reynolds, A. L. Dyer, F. C. Krebs, *J. Polym. Sci.* **2012**, *50*, 536.
[4] A. M. Österholm, D. E. Shen, D. S. Gottfried, J. R. Reynolds, *Adv. Mater. Technol.* **2016**, *1*, 1600063.
[5] J. Jensen, F. C. Krebs, *Adv. Mater.* **2014**, *26*, 7231.
[6] A. L. Dyer, E. J. Thompson, J. R. Reynolds, *ACS Appl. Mater. Interfaces* **2011**, *3*, 1787.
[7] P. Andersson, D. Nilsson, P. O. Svensson, M. Chen, A. Malmström, T. Remonen, T. Kugler, M. Berggren, *Adv. Mater.* **2002**, *14*, 1460.
[8] P. Andersson, R. Forchheimer, P. Tehrani, M. Berggren, *Adv. Funct. Mater.* **2007**, *17*, 3074.
[9] L. Gomes, A. Branco, T. Moreira, F. Feliciano, C. Pinheiro, C. Costa, *Sol. Energy Mater Sol. Cells* **2016**, *144*, 631.
[10] J. Padilla, A. M. Österholm, A. L. Dyer, J. R. Reynolds, *Sol. Energy Mater Sol. Cells* **2015**, *140*, 54.
[11] C. Pozo-Gonzalo, D. Mecerreyes, J. A. Pomposo, M. Salsamendi, R. Marcilla, H. Grande, R. Vergaz, D. Barrios, J. M. Sánchez-Pena, *Sol. Energy Mater Sol. Cells* **2008**, *92*, 101.
[12] A. A. Argun, A. Cirpan, J. R. Reynolds, *Adv. Mater.* **2003**, *15*, 1338.
[13] A. Malti, R. Brooke, X. Liu, D. Zhao, P. A. Ersman, M. Fahlman, M. P. Jonsson, M. Berggren, X. Crispin, *J. Mater. Chem. C* **2016**, *4*, 9680.
[14] P. Tehrani, L.-O. Hennerdal, A. L. Dyer, J. R. Reynolds, M. Berggren, *J. Mater. Chem.* **2009**, *19*, 1799.
[15] P. M. Beaujuge, S. Ellinger, J. R. Reynolds, *Nat. Mater.* **2008**, *7*, 795.
[16] P. Shi, C. M. Amb, E. P. Knott, E. J. Thompson, D. Y. Liu, J. Mei, A. L. Dyer, J. R. Reynolds, *Adv. Mater.* **2010**, *22*, 4949.
[17] W. T. Neo, C. M. Cho, Z. Shi, S.-J. Chua, J. Xu, *J. Mater. Chem. C* **2016**, *4*, 28.
[18] M. Içli, M. Pamuk, F. Algı, A. M. Önal, A. Cihaner, *Org. Electron.* **2010**, *11*, 1255.
[19] K.-R. Lee, G. A. Sotzing, *ChemComm* **2013**, *49*, 5192.
[20] G. Öktem, A. Balan, D. Baran, L. Toppare, *ChemComm* **2011**, *47*, 3933.
[21] C.-Y. Hsu, J. Zhang, T. Sato, S. Moriyama, M. Higuchi, *ACS Appl. Mater. Interfaces* **2015**, *7*, 18266.
[22] M. Sassi, M. M. Salamone, R. Ruffo, G. E. Patriarca, C. M. Mari, G. A. Pagani, U. Posset, L. Beverina, *Adv. Funct. Mater.* **2016**, *26*, 5240.
[23] H.-S. Liu, B.-C. Pan, D.-C. Huang, Y.-R. Kung, C.-M. Leu, G.-S. Liou, *NPG Asia Mater.* **2017**, 1.
[24] G. Sonmez, H. B. Sonmez, C. K. F. Shen, F. Wudl, *Adv. Mater.* **2004**, *16*, 1905.
[25] E. Unur, P. M. Beaujuge, S. Ellinger, J.-H. Jung, J. R. Reynolds, *Chem. Mater.* **2009**, *21*, 5145.
[26] S. V. Vasilyeva, J. R. Reynolds, P. M. Beaujuge, S. Wang, J. E. Babiarz, V. W. Ballarotto, *ACS Appl. Mater. Interfaces* **2011**, *3*, 1022.
[27] H. Shin, X. Yang, Y. Kim, T. Bhuvana, J. Lee, C. Park, E. Kim, *ACS Appl. Mater. Interfaces* **2012**, *4*, 185.
[28] Z. Xu, W. Wang, J. Wu, S. Mi, J. Zheng, C. Xu, *New J. Chem.* **2016**, *40*, 5231.
[29] A. M. Österholm, D. E. Shen, J. A. Kerszulis, R. H. Bulloch, M. Kuepfert, A. L. Dyer, J. R. Reynolds, *ACS Appl. Mater. Interfaces* **2015**, *7*, 1413.
[30] G. Wyszecki, W. S. Stiles, *Color Science: Concepts and Methods, Quantitative Data and Formulae*, John Wiley & Sons, New York, NY, **1982**.
[31] *Fea Hex Color Information Coca-Cola Red* **2011**, can be found under http://www.Spycolor.com/fe001a.
[32] P. M. Beaujuge, S. V. Vasilyeva, D. Y. Liu, S. Ellinger, T. D. McCarley, J. R. Reynolds, *Chem. Mater.* **2012**, *24*, 255.
[33] J. Schanda, in *Colorimetry Understanding the CIE System* (Ed.: J. Schanda), John Wiley & Sons, Hoboken, NJ **2007**, pp. 25–78.
[34] K. Cao, D. E. Shen, A. M. Österholm, J. A. Kerszulis, J. R. Reynolds, *Macromolecules* **2016**, *49*, 8498.
[35] J. A. Kerszulis, K. E. Johnson, M. Kuepfert, D. Khoshabo, A. L. Dyer, J. R. Reynolds, *J. Mater. Chem. C* **2015**, *3*, 3211.